EARTH SCIENCES

ISSN (Print): 24490954
ISSN (Online): 26364972

# GEOCHEMICAL PROXIES FROM CLAYS IN PARTS OF NORTHERN NIGER DELTA: IMPLICATION FOR UNRAVELLING PALEOWEATHERING AND PALEO-REDOX CONDITIONS

***[1]Osokpor, J. and [2]Osokpor, O.J.***

*[1]Department of Earth Sciences, Federal University of Petroleum Resources, PMB 1221, Effurun, Delta State, Nigeria*
*[2]Department of Geology, University of Benin, PMB 1154, Benin City, Edo State, Nigeria*

**Corresponding E-mail: Osokpor.jerry@fupre.edu.ng, jmobo@yahoo.com*

*Manuscript Received:17/11/2019 Accepted:29/01/2020 Published: March 2020*

**ABSTRACT**

Geochemical characterization of three clay occurrences in Igbanke, Esan and Asaboro area of Edo State were investigated for main oxides, minor and rare earth elements to unravel paleodepositional, source area past weathering condition. Inductively coupled plasma-optical emission spectrometry (ICP-OES) and inductively coupled plasma-mass spectrometry techniques were deployed to analyse the samples. $Al_2O_3$ and $Fe_2O_3$ depletion (13.63 - 30.46 wt. % and 0.38 – 5.09 wt. %) relative to $SiO_2$ (36.64 - 72.84 wt. %), close to the Post Achaean Australia shales and Upper Continental Crust standards of 62.8% and 66% respectively were recorded. Except Y, Zr, Hf, Ga, concentration of trace elements, are augmented relative to PAAS, although some samples show concentration ranges lower than or higher than average PAAS values. Redox-sensitive trace element proportions indicated variable paleo-redox conditions (oxic – suboxic), supported by negative cerium anomaly of -0.9 – -1.115. Low values of $K_2O/Al_2O_3$ (0.03 – 0.01) suggest a probable sedimentary reprocessing or intensification in the extent of source area weathering, affirmed by increase in $Al_2O_3$ and $Fe_2O_3$ values, a sign of weathering and geochemical modification. Observed depletion of $Na_2O$, MnO and CaO, besides quartz dilution, also indicates substantial weathering and sediment recycling, while lower concentration of $K_2O/Na_2O$ (4.0 - 8.5) indicates low dominance of albitic plagioclase, K-Feldspar, illite and mica.

**Keywords:** *Geochemical proxies, paleo-weathering, paleodepositional environment, paleo-redox, Niger Delta.*

## INTRODUCTION

Clays as sedimentary materials are widely distributed in time and space, and accounts for nearly half the volume of sedimentary rocks in the geological record and has many industrial uses. Therefore in both value and abundance it could be perceived as a foremost sedimentary mineral worldwide.

Clays are products of intense chemical weathering of pre-existing rocks. The chemically composition of clay stems from an intricate relationship of several variables, including source rock types and diagenesis, tectonic environment (Mehmet Muzaffer, 2013), and transportation processes, (Taylor and McLennan, 1985).

Clays constitute major part of soils, especially tropical soils as obtained in the area of study. Soils are formed under tropical climatic condition occasioned by high temperatures and humidity characterized by alternating dry and wet seasons which results in poor engineering properties (Maigien, 1966; Gidigasu, 1976; Charman 1988).

Considerable researches have been done on the geological nature of soil by various workers (Alabo and Pandy, 1987; Arumala and Akpokodje, 1987; Leton and Omotosho, 2004; Omotosho and Eze-Uzomaka, 2008). Ugbe (2011) studied the geotechnical properties of the clays in the area of study of this present work.

Although much work has been undertaken as it relates to the geotechnical nature of clays in southern Nigeria and the study area, not much has been done to unravel other geological parameters such as the paleoweathering and paleodepositional conditions prevalent during the formation of these clay bodies. The mineralogical and chemical composition of fine grained sediments indicates the influence of many different variables, e.g. provenance, climate, tectonics and weathering (Ahmad *et al.* 2014). Statistical evaluation of major, trace and minor elements present in sediments can be utilized in unravelling these variables.

Though there are geochemical ratios that are susceptible to oxidative alteration caused by weathering or diagenesis, so long as the bulk composition of the chemical constituents are not totally altered, important information can still be obtained from the geochemical composition of the sediments that can be applied to discriminate and unravel parameters such as provenance (Bakkiaraj *et al.,* 2010; Bhatia, 1983). Clays are assumed to represent crustal average composition of rock sources better than other sedimentary earth material (McCulloch and Wasserburg, 1978). Various geochemical signatures of rocks can thus be used to discuss and infer the paleo-weathering processes and the paleo-redox conditions which the sediments were subjected to during of their formation and maturity. This study seeks to apply bulk inorganic geochemical proxies to unravel the geological constraints prevalent during the formation of these clays from parts of Edo State, Nigeria. The geochemical aspect involves the determination of the rare earths elements (REE), trace and major elements, by X-ray florescence and inductive-coupled plasma-mass spectrometry techniques that would be statistically evaluated to determine the operative paleoweathering and paleo-redox environments during their formation.

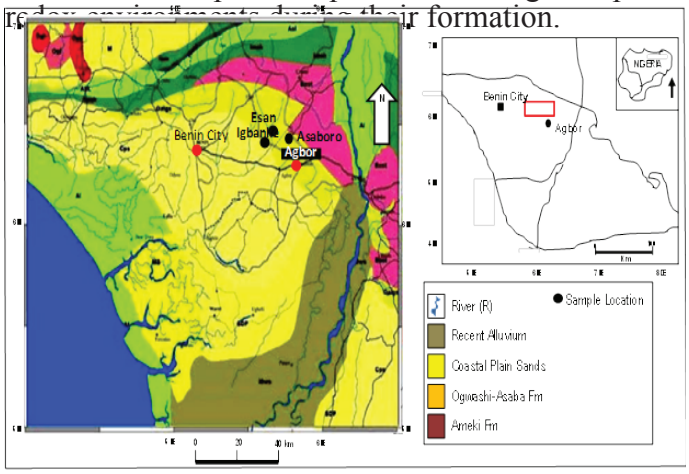


Figure 1: Geological map of western Niger Delta area showing field sampling locations sediments.

### Geology and Stratigraphy

The Niger Delta with an area of about 75, 000km$^2$ is situated in southern Nigeria along the West African coast and lies between longitudes 5° and 8°E and latitudes 3° and 6°N within the Gulf of Guinea. It has a total clastic fill of over 12,000 m (Short and Stauble, 1967). To the north is the Anambra Basin of Cretaceous age, the Calabar Flank and Abakaliki Anticlinorium located east and to the west, is the Benin Flank. The southern reaches merge with the Atlantic Ocean which forms its southern limit. It extends more than 300km from the proximal to distal ends and is presently building out into the Atlantic Gulf at the mouth of the Niger-Benue and Cross River drainage systems (Reijers, 1996). Progradational and regressive deposition characterize the delta sequence, although a net progradation southwards since Eocene to Recent, has seen the delta forming successive depositional tracts that represent the newest depositional area of the delta formation at each stage of its growth (Whiteman, 1982, Reijers, 1996).

The tectonic history and the nascent stratigraphic emergence Delta is related to the tectono-sedimentary evolution and development of the Benue Trough, which evolved during the Early Cretaceous a resultant product of the drifting of South American from the African Continent in the Late Jurassic – Early Cretaceous times.

Threeage-diachronousmainLithostratigraphic formations, the Akata, Agbada and Benin Formations are recognized in the Niger Delta (Short and Stauble, 1967), although older lithostratigraphic packages, the Imo Shale, Ameki and Ogwashi-Asaba Formations, are present in the northern parts of the basin and range in age from Eocene to Oligocene (Short and Stauble, 1967; Avbovbo, 1978; Whiteman, 1982). The Akata Formation is composed of 90 % + prodelta marine shale and less than 10% of sandstone and occurs as the bottomset, with a thickness in excess of 6000m. It has a diachronous age range of Eocene to Recent. Unconformably overlying the Akata Formation is the Agbada Formation, is composed of sand and shale

of delta front origin. These sandy lithofacies were formed in shoreface and channel subenvironments with minor shale and an alternation of sand and shale of almost equal proportion in the lower part the delta foreset. It has a thickness range of about 3000m to 4500m, and an Eocene to Recent age. The Benin Formation contains over 90% terrestrial sands and coarser sediments interbedded with finer grained sediments like clay and silts formed in a delta plain environment. The thickness is variable, and generally exceeds 2100m and with an age range of Oligocene – Recent (Whiteman, 1982, Nwajide, 2013).

The Ogwashi-Asaba Formation (Whiteman, 1982; Okezie and Onuogu, 1985), earlier termed the Lignite Series (Parkinson, 1907) is composed of clay, sand, shale and lignite and represent stratigraphic units of Oligo-Miocene age overlying the Ameki Group. In areas where detailed studies has been done on the formation (Okezie and Onuogu, 1985), they are observed to present in the Nanka Formation (Ameki Group facies) around the Nnewi-Oba area, whereas the Benin Formation hosts the lignites in the Ikot-Ekpene area, implying Formation is transformational occurrence of the lignites.

### *Study Locations and Outcrop Description*

This study was undertaken in the proximal areas of the Niger Delta and involved the sampling of surficial deposits from outcrops on road cuts and river channel banks. Five locations from three areas were sampled for this study and includes, Asaboro, Igbanke (Ugo and Oguoguo) and Esan (Ewohimi, Atari and Ekpon) areas east of Benin City (Fig. 1), within Latitudes N06°16′32.2′′ - N06°26′29.6′′ and Longitudes E006°2′12.6′′ - E006°21′00.6'' for the Asaboro Quarry and Latitudes N06°23′ - N6°30′ and Longitudes E006°18′ - E006°2′ for the Ewohimi area respectively (Fig. 1). In terms of structuro-stratigraphic domain, the area of study is located within the northern depositional belt of the Niger Delta, and is underlain by of Oligocene age sediments of the Ogwashi-Asaba Formation and the Coastal Plain sands (Benin Formation) (Short and Stuable, 1967, Whiteman, 1982). The sediments are characterized by basal clays units which probably grades imperceptibly into finer grain sand facies in the subsurface and overlain by horizons of reddish-brown very fine and pebbly sandy clays and clayey sand with thickness range 9.5 to 13 meters. The sands are in turn overlain by surficial weathered and slightly consolidated clayey sands (top soil). The surficial sediments exhibit reddish colouration, a product of long periods of tropical climatic weathering. The weathered horizon has thickness of up to four meters in places.

## MATERIALS AND METHODS

### *Geochemical Analytical Procedures*

### *Sample Preparation*

The clay samples obtained from the field were air-dried and 25g of each sample was weighed out, using a high tech Mettler Toledo PL602-S electrical weighing balance, at the Earth Sciences Geology Laboratory, University of Petroleum Resources, Effurun, Nigeria. During preparation for analysis, the samples were dried at 60°C and pulverized to 85% passing 200 mesh (75 microns), using a mild-steel pulverizer (PUL85). The weighed samples were prepared and analysed for quantitative elemental compositions.

### *Trace Elements Analysis: Inductively Coupled Plasma-Mass Spectrometry (ICP-MS)*

After preparation, 10g of each sample was dissolved to complete dryness with a 2:2:1:1 $H_2O$-HF-$HClO_4$-$HNO_3$ acid solution. 50% hydrogen chloride solution was then added to the filtrate and heated with a mixing hot block (Kowal-Linka, 2014). The solutions were poured into test tubes after cooling, and dilute HCl added to bring to volume (Kowal-Linka, 2014). 0.25g of each sample were investigated for the concentrations of trace using ICP-OES (Inductively Coupled Plasma-Optical Emission Spectrometry). The analysis (ICP-OES) was performed with the NexION® 300 ICP-MS instrument.

Quality Assurance (QA) and Quality control (QC) were applied in the sample analyses using Nickel Sulphide Ore (OREAS 72b) and Geochemical Multi-acid Digestion (OREAS 45E) reference materials as standards to ensure accuracy of results.

### *Major Element Analysis: X-Ray Fluorescence Spectrometry (XRF)*

Major element analysis of the clay samples was achieved by roasting a fixed quantity of each sample to initially define Loss on Ignition (LOI) before the XRF analysis (Alaku, *et al.,* 2017). After roasting, the samples were then attached in a platinum-gold receptacle with a commercial Lithium Tetraborate ($LiBO_4$) flux (Olufemi *et al.,* 2018). Furthermore, the melted solid was cast in a platinum mould and the fused discs investigated (Olufemi *et al.,* 2018), for main elements by an X-Ray fluorescence spectrometer (Varghese, 2018). QA and QC of analytical results were done using a Diorite Gneiss (SY-4) reference material as a standard.

### *Geochemical Statistical Analysis*

Statistical analyses of geochemical data were done with Microsoft Excel (version 2013). Discriminant function analysis was performed to obtain a terrigeneous sandstone and shale classification diagram (Mishra, 2010); the A-CN-K Ternary diagram of Nesbitt and Young (1984; 1989). Post Achaean Australian Shale (PAAS) normalization of trace elements were performed and the plots generated with Microsoft Excel. Also, plots of indices of chemical alteration (CIA) versus $SiO_2$, Zr/Sc versus $SiO_2$, V/Cr versus Ni/Co, V/V+Ni versus Ni/Co and major elements versus $Al_2O_3$ were also generated with Microsoft Excel. Normalization was done by dividing the elemental concentrations of the samples by the concentrations of PAAS and Chondrite respectively.

## RESULTS AND DISCUSSION

### *Elemental Composition and Variation*

Results of the bulk geochemistry are shown in Tables 1 and 2. Table 1 presents the bulk Major Element's composition and concentrations values compared

to PAAS (Ngueutchoua *et al.,* 2017) and Upper Continental Crust (UCC) (Taylor and McLennan, 1985). Table 2 presents quantitative Trace Elemental concentration and composition of the clay samples and the PASS (Yongjie *et al.,* 2017).

The clays are depleted in $Al_2O_3$ and $Fe_2O_3$ (13.63 - 30.46 wt. % and 0.38 – 5.09 wt. % respectively) relative to $SiO_2$ (36.64 - 72.84 wt. %), which is close to the Post Archean Australia shales (PAAS) and UCC values of 62.8% and 66% respectively. A lower concentration of $K_2O/Na_2O$ (4.0 - 8.5) indicates low dominance of albitic plagioclase, K-Feldspar, illite and mica (Ikhane, 2014; Mishra and Sen, 2012). The very low values of $K_2O/Al_2O_3$ (0.03 – 0.01) suggest a probable secondary recycling of sediments or intensification of weathering in the source area (Ikhane, 2014). This can be supported by the increase in the $Al_2O_3$ and $Fe_2O_3$ values (Table 1), indicating weathering and geochemical alteration (Ikhane, 2014). The high value of $SiO_2/Al_2O_3$ (1.20–5.34) indicates quartz enrichment (Bhatia, 1983).

Other major elements ($Na_2O$, $k_2O$, MnO, MgO, $P_2O_5$, $Cr_2O_5$ and $CaO_)$ are heavily depleted with a very low average compared to PAAS and UCC values, except for TiO2 which range from 1.03 - 3.09 wt. % in all the samples. The $K_2O/Al_2O_3$ ratios for clay minerals and feldspar minerals are 0.0 - 0.3 and 0.3 - 0.9 respectively. The detected reduction in $Na_2O$, MnO and CaO (Akarish, and El-Gohary, 2011), besides quartz dilution, also indicates that the sediments have suffered substantial weathering and sediment recycling (Joo *et al.,* 2005; Jin *et al.,* 2006).

In the bivariate plot (Fig. 2), $TiO_2$, and $P_2O_5$, has a positive correlation with $Al_2O_3$, $SiO_2$ is negatively correlated, while the other oxides had no correlation with the $Al_2O_3$, indicating that $SiO_2$ was contributed to the clays and the other oxides were not originally associated with the clay minerals. Also, the CaO may be from a carbonate source.

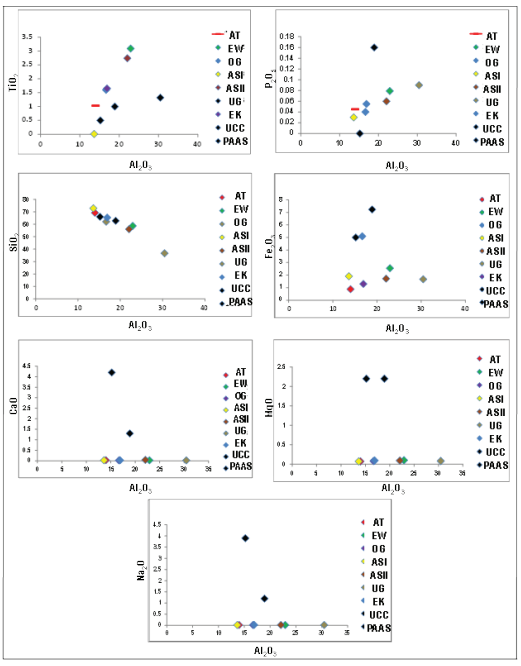


Figure 2: Bivariate plot of $Al_2O_3$ versus oxides of other major elements

Table 1: Composition and concentrations of major elements in the analysed samples compared to PAAS and UCC values.

| Oxide % (Wt. %) | Detection Limit | Esan Clay | | | Asaboro Clay | | Igbanke Clays | | Average Esan Clay | Average Asaboro Clay | Average Igbanke Clays | UCC | PAAS |
|---|---|---|---|---|---|---|---|---|---|---|---|---|---|
| | | AT | EW | EK | ASI | ASII | UG | OG | | | | | |
| $SiO_2$ | 0.01 | 69.20 | 58.7 | 65.28 | 72.84 | 56.03 | 36.64 | 62.05 | 64.39 | 64.44 | 49.35 | 66.00 | 62.80 |
| $Al_2O_3$ | 0.01 | 14.0 | 22.92 | 16.90 | 13.63 | 22.07 | 30.46 | 16.67 | 17.94 | 17.85 | 23.57 | 15.20 | 18.90 |
| $Fe_2O_3$ | 0.01 | 0.88 | 2.55 | 1.30 | 1.91 | 1.72 | 1.67 | 5.09 | 1.58 | 1.82 | 3.38 | 5.00 | 7.23 |
| CaO | 0.01 | 0.03 | 0.024 | 0.025 | 0.025 | 0.043 | 0.019 | 0.021 | 0.03 | 0.03 | 0.02 | 4.20 | 1.30 |
| MgO | 0.01 | 0.07 | 0.1 | 0.09 | 0.07 | 0.09 | 0.08 | 0.08 | 0.09 | 0.08 | 0.08 | 2.20 | 2.20 |
| $Na_2O$ | 0.01 | <0.02 | <0.02 | <0.02 | <0.02 | <0.02 | <0.02 | <0.02 | 0.02 | 0.02 | 0.02 | 3.90 | 1.20 |
| $K_2O$ | 0.01 | 0.08 | 0.14 | 0.17 | 0.05 | 0.16 | 0.16 | 0.08 | 0.13 | 0.11 | 0.12 | 3.40 | 3.70 |
| MnO | 0.01 | 0.006 | 0.014 | 0.008 | 0.006 | 0.012 | 0.002 | 0.011 | 0.01 | 0.01 | 0.01 | 0.08 | 0.11 |
| $TiO_2$ | 0.01 | 1.03 | 3.09 | 1.65 | 0.01 | 2.74 | 1.32 | 1.60 | 1.92 | 1.36 | 1.46 | 0.50 | 1.00 |
| $P_2O_5$ | 0.01 | 0.045 | 0.079 | 0.055 | 0.03 | 0.06 | 0.09 | 0.04 | 0.06 | 0.04 | 0.07 | ND | 0.16 |
| $Cr_2O_3$ | 0.01 | 0.01 | 0.02 | 0.01 | 0.01 | 0.02 | 0.02 | 0.02 | 0.01 | 0.02 | 0.02 | ND | ND |
| LOI | ND | 13.9 | 11.18 | 14.35 | 8.79 | 16.66 | 28.89 | 14.26 | 13.14 | 12.73 | 21.58 | ND | ND |
| SUM | ND | 99.27 | 98.84 | 99.86 | 97.39 | 99.63 | 99.37 | 99.94 | 99.32 | 98.51 | 99.67 | | 98.60 |
| $Al_2O_3/TiO_2$ | ND | 13.59 | 7.42 | 10.24 | 1363 | 8.06 | 23.08 | 10.42 | 10.42 | 12.98 | 16.75 | 30.40 | 18.90 |
| CIA | ND | 99.29 | 99.31 | 98.89 | 99.49 | 99.19 | 99.41 | 99.40 | 99.33 | 99.30 | 99.41 | 57.58 | 75.60 |
| CIW | ND | 99.86 | 99.91 | 99.88 | 99.85 | 99.91 | 99.93 | 99.88 | 99.88 | 99.89 | 99.91 | 66.09 | 88.73 |
| PIA | ND | 100.43 | 100.53 | 100.90 | 100.22 | 100.64 | 100.46 | 100.36 | 100.62 | 100.48 | 100.41 | 60.20 | 86.36 |
| $Na_2O/K_2O$ | ND | 0.25 | 0.14 | 0.12 | 0.4 | 0.13 | 0.13 | 0.25 | 0.17 | 0.19 | 0.19 | 1.14 | 0.32 |
| $SiO_2/Al_2O_3$ | ND | 4.94 | 2.56 | 3.86 | 5.34 | 2.54 | 1.20 | 3.72 | 3.59 | 3.61 | 2.09 | ND | ND |

PAAS: *Post Achaean Australian Shale; UCC: Upper Continental Crust, ND: Not Determined; CIA: Chemical Index of Alteration; CIW: Index of Chemical Weathering; PIA: Plagioclase Index of Weathering; AT: Atari, EW: Ewohimi, EK: Ekpon, ASI: Asaboro I, ASII: Asaboro II, OG: Oguoguo, UG: Ugo*

Table 2: PAAS-Normalized Trace Elements Concentration of Esan, Asaboro and Igbanke Clays and the PAAS values

| Element | Detection Limit (ppm) | AT | EW | EK | ASI | ASII | OG | UG | Range | Average Esan Clay | Average Asaboro Clay | Average Igbanke Clay | PAAS |
|---|---|---|---|---|---|---|---|---|---|---|---|---|---|
| La | 0.1 | 61.60 | 32.10 | 56.10 | 84.10 | 35.60 | 44.50 | 53.00 | 32.1 – 84.1 | 49.93 | 59.85 | 48.75 | 38 |
| Y | 0.1 | 14.90 | 6.10 | 12.60 | 13.70 | 10.6 | 15.30 | 16.00 | 6.1 – 16.0 | 11.20 | 12.15 | 15.65 | 27 |
| Zr | 0.2 | 195.40 | 136.90 | 317.90 | 324.00 | 102.70 | 350.10 | 247.50 | 102.7 – 350.1 | 216.73 | 213.35 | 298.8 | 210 |
| Ba | 1 | 115.00 | 48.00 | 166.00 | 148.00 | 82.00 | 156.00 | 118.00 | 48 - 166 | 109.67 | 115.00 | 137.00 | 650 |
| Hf | 0.02 | 5.45 | 4.12 | 8.49 | 9.68 | 3.32 | 10.40 | 6.96 | 3.32 – 10.4 | 6.02 | 6.5 | 8.68 | 5 |
| Sc | 0.1 | 6.70 | 7.00 | 8.20 | 8.80 | 9.60 | 10.10 | 9.60 | 6.7 – 10.1 | 7.30 | 9.2 | 9.85 | 16 |
| Cr | 1 | 29.00 | 39.00 | 90.00 | 6.10 | 50.00 | 104.00 | 64.00 | 29 – 104 | 52.67 | 55.50 | 84 | 110 |
| Sr | 1 | 36.00 | 27.00 | 88.00 | 68.00 | 46.00 | 69.00 | 67.00 | 36 – 88 | 50.33 | 57.00 | 68 | 200 |
| V | 1 | 47.00 | 81.00 | 125.00 | 116.00 | 99.00 | 109.00 | 117.00 | 47 – 125 | 84.33 | 107.50 | 113 | 150 |
| Ni | 0.1 | 6.70 | 16.00 | 19.90 | 12.00 | 10.10 | 21.80 | 20.80 | 6.7 – 21.8 | 14.20 | 11.05 | 21.3 | 55 |
| Co | 0.2 | 1.40 | 2.20 | 3.10 | 2.40 | 3.30 | 3.40 | 3.00 | 1.4 – 3.4 | 2.23 | 2.85 | 3.2 | 23 |
| Zn | 0.2 | 10.70 | 14.50 | 27.10 | 15.60 | 13.60 | 23.60 | 20.30 | 10.7 – 27.1 | 17.43 | 14.60 | 21.95 | 85 |
| Cu | 0.02 | 3.34 | 6.43 | 7.34 | 7.60 | 8.48 | 8.99 | 10.89 | 3.34 – 10.89 | 5.70 | 8.04 | 9.94 | 50 |
| Ga | 0.02 | 14.64 | 17.04 | 36.28 | 27.21 | 24.16 | 35.81 | 30.14 | 14.64 – 36.38 | 22.65 | 25.69 | 32.98 | 20 |
| Rb | 0.1 | 4.30 | 2.30 | 14.90 | 5.20 | 7.60 | 6.50 | 6.70 | 2.3 – 14.9 | 7.17 | 6.40 | 6.6 | 160 |
| Nb | 0.04 | 29.31 | 30.77 | 81.13 | 68.29 | 32.16 | 81.81 | 58.86 | 29.31 – 81.13 | 47.07 | 50.23 | 70.34 | 19 |
| Pb | 0.02 | 30.22 | 21.43 | 42.01 | 52.14 | 28.91 | 33.44 | 39.66 | 21.43 – 52.14 | 31.22 | 40.53 | 36.55 | 20 |
| Th | 0.1 | 13.10 | 14.60 | 18.20 | 23.00 | 23.80 | 18.90 | 18.70 | 13.1 – 23.8 | 15.00 | 23.40 | 18.8 | 14 |
| U | 0.1 | 2.50 | 2.20 | 4.20 | 4.50 | 6.40 | 5.00 | 3.60 | 2.2 – 6.4 | 2.97 | 5.45 | 4.3 | 3.1 |
| Th/U | - | 5.24 | 6.636 | 4.333 | 5.111 | 3.719 | 3.780 | 5.194 | 3.78 – 6.636 | 5.403 | 4.42 | 4.487 | 4.52 |
| V/Cr | - | 1.621 | 2.077 | 1.389 | 1.902 | 1.980 | 1.048 | 1.828 | 1.048 – 2.077 | 1.696 | 1.941 | 1.438 | 1.36 |
| Ni/Co | - | 4.786 | 7.273 | 6.419 | 5.000 | 3.061 | 6.412 | 6.933 | 3.061 – 7.273 | 6.159 | 4.031 | 6.673 | 2.39 |
| Zr/Sc | - | 29.164 | 8.556 | 15.975 | 27.000 | 10.168 | 16.060 | 11.899 | 8.556 – 29.164 | 17.898 | 18.584 | 13.980 | 0.59 |
| V/V+Ni | - | 7.015 | 5.063 | 6.281 | 9.667 | 9.802 | 5.000 | 5.625 | 5.00 – 9.802 | 6.120 | 9.735 | 5.313 | 0.73 |

*AT: Atari, EW: Ewohimi, EK: Ekpon, ASI: Asaboro I, ASII: Asaboro II, OG: Oguoguo, UG: Ugo*

Concentrations trace elements in each sample was normalized by PAAS values (Pundaree *et al.,* 2015) (Table 2) and are plotted in the multi-element diagram (Fig. 3).

Modal trace elements concentration, with the exemption of Y, Zr, Hf and Ga in the samples are enriched relative to PAAS, although some samples from specific locations show concentration ranges lower than or higher than average PAAS values. Th (13.1 ppm.), Zr (195.4 ppm.), U (2.50), and Ga (14.64 ppm.) are depleted in sample Atari. La (32.1), Hf (4.12), Zr (136.9) and U (2.200) are depleted in Ewohimi sample. La (35.6), Hf (3.32) and Zr (102.7) are depleted in Asaboro sample II.

The average concentration values of La, Zr and Hf in the samples from the three study areas (Esan, Asaboro and Igbanke) indicate marked enrichment relative to average PAAS values which are 38 ppm, 210 ppm and 5 ppm, respectively for these elements. While U is on average, depleted in the Esan Clays, and increased in the Asaboro and Igbanke samples relative to the PAAS.

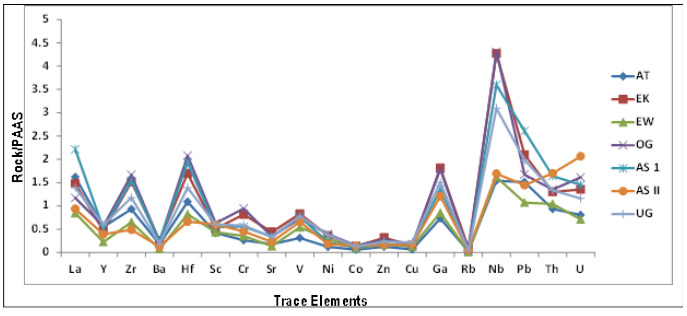


Figure 3: Multi-element diagram showing the PAAS-normalized Trace element distribution pattern of the samples (after Taylor and Mclennan, 1981)

### *Geochemical Classification*

From the data set presented in Table 1, the samples were classified based on the composition of major elements using the plot of Fe2O3/K2O vs. $SiO_2/Al_2O_3$ on the Terrigeneous sandstone and shale diagram (Fig. 4) of Herron (1988). From the plot it can be deduced that the clays are impure clays. The Igbanke clays are iron rich. While most of the samples plot within the Fe Shale field, two samples from the Esan and Asaboro area plot inside the Fe sand field. In reality these samples are not sand, but rather high in sand percentage, which substantially influenced its geochemical attributes.

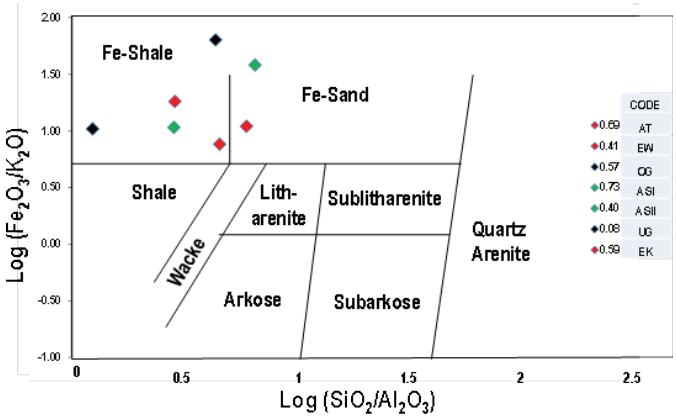


Figure 4: Classification of Terrigeneous Sandstones and Shales (After Herron, 1988)

### *Paleoweathering Index*

The extent of chemical weathering can be well determined and measured by the calculation of weathering indices such as CIA, (Nesbitt and Young, 1982); CIW, (Harnois, 1988) and Plagioclase

Index of Alteration (PIA), (Fedo *et al.* 1995) (Table 1). The CIA is defined as CIA=[$Al_2O_3$/($Al_2O_3$+CaO*+NaO+$K_2O$)]×100 (Ngueutchoua *et al.* 2017); the CIW is defined as CIW=[$Al_2O_3$/($Al_2O_3$+CaO*+NaO)]×100, while the index of plagioclase alteration (PIA) is defined as PIA=[$Al_2O_3$/($Al_2O_3$+CaO*+NaO–$K_2O$)]×100.CaO* in the equations given above, is the quantity of incorporated CaO in the silicate minerals of the studied samples (Fedo *et al.,* 1995). Carbonate contribution Correction for CaO was not done for the studied samples due to the unavailability of $CO_2$ data. Hence, computation for CaO* from the silicate fraction, an assumption was adopted proposed by Bock et al. (1998). Thus, CaO values were used in the equations only if CaO≤$Na_2O$; hence, when CaO>$Na_2O$, it was taken that the concentration of CaO was same as $Na_2O$ (Bock *et al.,* 1998).

Kaolinite has a value of 100 in the Chemical Index of alteration scale which represents the maximum grade of weathering. Illite ranges from 75 and 90. Muscovite has a value of 75, the feldspars have 50. Newly formed basalts have values which range from 30 and 45, while unweathered granites and granodiorites have values between 45 and 55 (Bahlburg and Dobrzinski, 2011). In the CIA versus $SiO_2$ plots, (Fig. 56), the positions of the samples suggests sediments of the PAAS have been intensely weathered as they plot in the domain of illite and muscovite unlike the UCC which falls slightly above the region of feldspars and has relatively not undergone intense weathering. Higher SiO2 concentration in the shales, PAAS and UCC, however, indicates a higher amount of reworking of these sediments compared to some of the samples.

Intense weathering of the samples is also supported by the high CIW values which range averagely between 99.92 - 99.89 (Table 1) and in agreement with the high CIA values. The classification of weathering profiles (Nesbitt and Young, 1989), displayed on an A-CN-K ternary diagram (González *et al.,* 2017) (Fig. 6) demonstrates that all the samples plot within the kaolinite, gibbsite and chlorite domain of the diagram. This indicates and further affirms that the samples have been subjected to intense weathering.

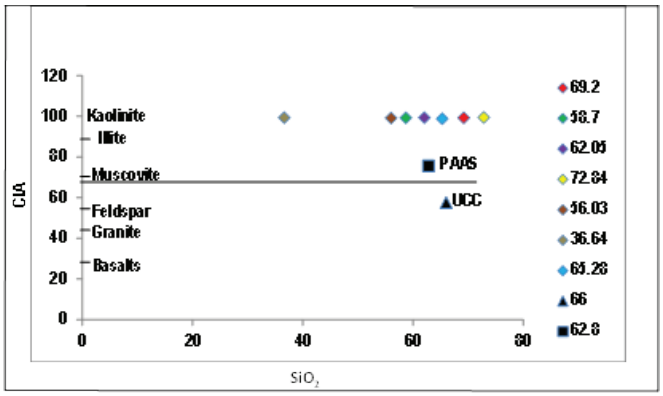


Figure 5: A binary plot of CIA-SiO2 (after Nesbitt & Young, 1982)

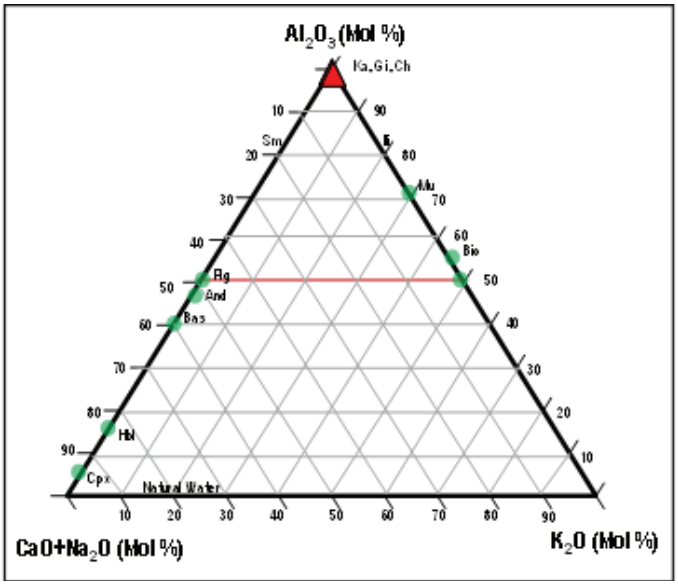


Figure 6: Weathering profiles of the samples plotted on an $Al_2O_3$-CaO+$Na_2O$-$K_2O$ (A-CN-K) Ternary diagram (after Nesbitt and Young, 1984; 1989). (Ka: kaolinite; Ch: chlorite; Ill: illite; Sm: Smectite; Cpx: clinopyroxene; Hbl: Hornblende; Plg: Plagioclase; Mu: muscovite; Bio: biotite; Ks: potassium feldspar; Gi: gibbsite; Bas: basalt; And: andesite)

### *Paleo-Redox Condition*

Ratios of Redox-sensitive trace element (Ni/Co, V/V+Ni and V/Cr) (Ikhane, 2014) (Table 2) are commonly considered potent geochemical indicators for paleoenvironmental typing (Ngong *et al.,* 2015). Zeng *et al.,* (2015) proposed that oxic a condition is inferred when Ni/Co ratios < 5, dysoxic conditions when the values range from 5–7, and suboxic to anoxic conditions when values are > 7. They also suggested that values of V/Cr ratios < 2 inferred oxic conditions (Ikhane 2014), values between 2 – 4.25 indicated dysoxic conditions, while values > 4.25 indicates suboxic to anoxic conditions (Rimmer, 2004). (Rimmer, 2004) presented values of V/V+Ni greater than 0.5 to have been derived from organic matter formed under euxinic conditions. Also a comparison of V/V+Ni ratios to other geochemical redox indicators, which included the degree of pyritization by Hatch and Leventhal (1992), suggested that values greater than 0.84 indicated euxinic bottom water condition, 0.54-0.82 anoxic water conditions and 0.46-0.60 for dysoxic conditions (Šajnović *et al.,* 2019).

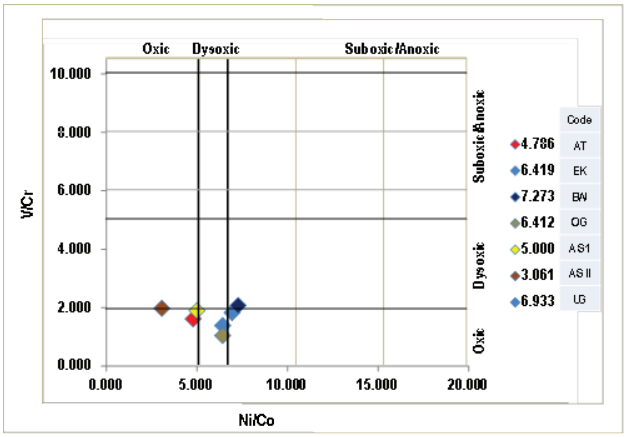


Figure 7: Redox-sensitive trace metal ratios V/Cr versus Ni/Co cross plots. Ranges obtained from Jones and Manning (1994)

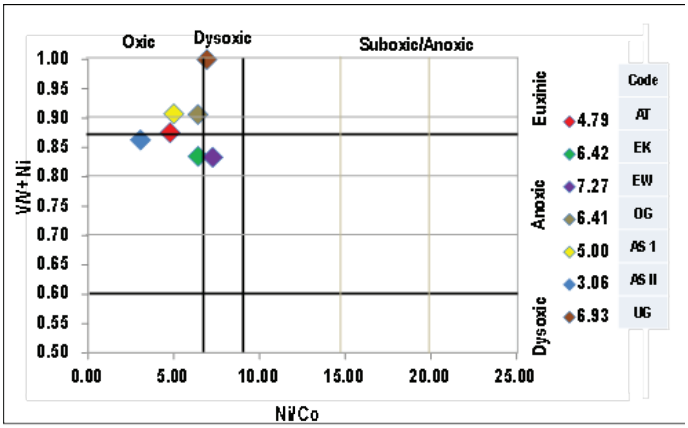


Figure 8: Redox-sensitive trace metal V/(V+Ni) versus Ni/Co ratios cross plots. Ranges are obtained from Ikhane, 2014 and Moradi, 2016.

As shown above, samples UG and OG and samples EK and EW falls within the dysoxic and suboxic region of the Ni/Co axis respectively, while others fall within the oxic region of the cross plot. However in figure 8, a change is notice as sample EW that initially plotted in the suboxic region now plots in the dysoxic domain, while sample UG remained unchanged. These two cross plots are largely correlated, as the V/V+Ni cross plot further strengthened the interpretation derived from figure 9 (V/Cr vs Ni/Co). This is supported by the negative cerium anomaly of the samples (-0.9 – -1.115), (Wilde *et al.,*1996).

## CONCLUSIONS

Whole rock geochemical data of clay samples obtained from surface exposures located in Igbanke, Esan and Asaboro areas of Edo State located in southern Nigeria, revealed a predominance of $Al_2O_3$ and $Fe_2O_3$ over other oxides, although depleted relative to $SiO_2$, which is close to the Post Archean Australia shales (PAAS) and UCC. Other major elements ($Na_2O$, $k_2O$, MnO, MgO, $P_2O_5$, $Cr_2O_5$ and CaO) are also heavily depleted with a very low average compared to PAAS and UCC values, except for $TiO_2$ which higher values all the samples. Statistical ratios of $K_2O/Na_2O$, indicate low dominance of albitic plagioclase, K-Feldspar, illite and mica. As $Al_2O_3$ is a characteristic feature of feldspars and $TiO_2$ in mafic minerals, the $Al_2O_3/TiO_2$ ratio (Fatehi and Ahmadipour, 2018), indicates the rocks were sourced from a felsic source, ascertained by the low values of MgO (Mishra, 2010).

Very low $K_2O/Al_2O_3$ values suggest a probable sedimentary reworking or weathering intensification in the source area, supported by the increase in the $Al_2O_3$ and $Fe_2O_3$ values which are indication of weathering and geochemical alteration. The high value of $SiO_2/Al_2O_3$ indicates quartz enrichment.

The $K_2O/Al_2O_3$ ratios for clay minerals and feldspar minerals are 0.0 - 0.3 and 0.3 - 0.9 respectively. The observed depletion in $Na_2O$, MnO and CaO, besides quartz dilution, indicates that the sediments have suffered substantial weathering and sediment recycling. Comparison of values derived from this study with published data revealed an oxic to suboxic paleodepositional environment, intense paleo-weathering, sediment recycling and a felsic cratonic provenance for the clays.

## REFERENCES

Ahmad AHM, Noufal KN, Alam M & Masroor Tavheed Khan 2014. Petrography and geochemistry of Jumara Dome sediments, Kachchh Basin: Implications for provenance, tectonic setting and weathering intensity, *Chinese Journal of Geochemistry, 33: 9–23*.

Akarish AIM & El-Gohary AM 2011. "Provenance and Source Area Weathering Derived from the Geochemistry of Pre-Cenomanian Sandstones, East Sinai, *Egypt, Journal of Applied Sciences, 11(17): 3070-3088.*

Alabo EH & Pandy P 1987. Distribution of engineering properties of red soils in the central Lower Niger Delta, Nigeria. *9th African Reg. Conf. Soil Mechanics and Found. Engrg, Lagos, 49-55.*

Alaku I, Moshood O, Agbor A & Alabi A 2017. Geochemical Characteristic and Petrogenesis of Malumfashi Schist around Tandama Area, North-Western Nigeria, *British Journal of Applied Science & Technology, 20(1): 1-14.*

Arumala JO & Akpokodje EG, 1987. Soil properties and pavement performance in the Niger Delta. Q. *J. Eng. Geol., 20: 287-296.*

Avbovbo AA 1978. Tertiary lithostratigraphy of Niger Delta. AAPG Bull., 62(2): 295-306.

Bakkiaraj D, Nagendra R, Nagarajan R, & Armstrong-Altrin JS 2010. Geochemistry of sandstones from the Upper Cretaceous Sillakkudi Formation, Cauvery Basin, Southern India:Implication for provenance. *Journal of the Geological Society of India, 76: 453-467.*

Bahlburg, H. and Dobrzinski, N., 2011. A Review of the Chemical Index of Alteration (CIA) and Its Application to the Study of Neoproterozoic Glacial Deposits and Climate Transitions. – In: Arnaud, E., Halverson, G. P., Shields Zhou, G. A. (eds.) The Geological Record of Neoproterozoic Glaciations. Memoir 36: 81–92. Geological Society, London.

Bamigboye OS, Adekeye JID, Kadioglu YK, Adeonipekun D & Omorinoye OA 2018.Geochemistry and origin of Fe-Mn oxide mineralization in Kaoje- Derena and their environs, northwestern Nigeria, *Arabian Journal of Geosciences, 11(19): 1-18.*

Bhatia MR 1983. Plate tectonics and geochemical composition of sandstones: *Journal of Geology,91:611-627.*

Bock B, McLennan SM, Hanson GN 1998. Geochemistry and provenance of the Middle Ordovician Austin Glen Member (Normanskill formation) and the Taconian Orogeny in New England. *Sedimentology. 45:635–655*

Burke KCA, Dessauvagie, TFJ & Whiteman AJ 1971. Openning of the Gulf of Guinea and the Geological History of the Benue Depression and Niger Delta. Nature, 233: 51-55.

Burke KCA, Dessauvagie TFJ & Whiteman, AJ 1972. Geological history of the Benue valley and adjacent areas. In: Dessauvagie, TFJ and Whiteman, A J (eds). African Geology. Univ. Ibadan, 187-205.

Chairman JH 1988. Laterite in road pavements. Construction Industry Research and Information Association (CIRCA), special publication 47, West Minister, London.

Cratchley CR, & Jones G P 1965. An interpretation of geology and gravity anomalies of the Benue Valley, Nigeria. *Overseas Geology Surv. Geophysics paper. 11:26p.*

Fatehi H. & Ahmadipour H 2018. Geochemistry and petrogenesis of metabasites from the Gol- e-Gohar Complex in southern Sanandaj-Sirjan metamorphic zone, South of Iran; Evidences for crustal extension and magmatism at early. *Geologica Acta, 16(3): 293-319*

Fedo CM, Nesbitt HW, & Young GM 1995. Unraveling the effects of potassium metasomatism in sedimentary rocks and paleosols, with implications for paleo weathering conditions and provenance. Geology. 23: 921–924.

Gidigasu MD 1976. Lateritc Soil Engineering. Elsevier Scientific Publishing Co, New York. Grant NK 1971. South Atlantic, Benue Trough and Gulf of Guinea Cretaceous triple Junction. *Geol. Soc. Amer. Bull. 82: 2295-2298.*

González PAA, Garban G, Hauser N & Gigena L 2017. Geochemistry of metasedimentary rocks from the Puncoviscana Complex in the Mojotoro Range, NW Argentina: Implications for provenance and tectonic setting, *Journal of South American Earth Sciences. 78:250-263.*

Harnois L (1988). The new index, a new chemical index of weathering. *Sedimentary Geology, 55: 319-322.*

Hatch JR & Leventhal JS 1992. Relationship between inferred redox potential of the depositional environment and geochemistry of the Upper Pennsylvanian (Missourian) stark shale member of the Dennis Limestone, Wabaunsee County, Kansas, USA. *Chemical Geology, 99: 65-82.*

Herron MM 1988. Geochemical classification of terrigenous sands and shales from core or log data. *J. Sed. Petrol., 58: 820–829.*

Ikhane RP, Akintola AI, Bankole SI & Oyinboade YT 2014. Provenance Studies of Sandstone Facies Exposed Near Igbile Southwestern Nigeria: Petrographic and Geochemical Approach, *Journal of Geography and Geology,6: 47-68.*

Jin Z, Cao J, Wu J & Wang S 2011. A Rb/Sr record of catchment weathering response to Holocene climate change in Inner Mongolia. Earth Surface Processes and Landforms. DOI: 10.1002/esp.1243

Jones B & Manning DAC (1994). Comparison of geochemical indices used for the interpretation of palaeoredox conditions in ancient mudstones. *Chemical Geology, 111: 111-129.*

Joo Y Ji, Lee YI & Bai TZ 2005. Provenance of the Qingshuijian formation (Late Carboniferous), NE China: implications for tectonic processes in the northern margin of the North China block. *Sediment. Geol., 177: 97–114.*

Kowal-Linka M, Jochum KP, Surmik D 2014. LA-ICP-MS analysis of rare earth elements in marine reptile bones from the Middle Triassic bonebed (Upper Silesia, S Poland): Impact of long-lasting diagenesis, and factors controlling the uptake, *Chemical Geology. 363:213–228.*

Leton TG & Omotosho O 2004). Landfill operations in the Niger Delta region of Nigeria.Eng. Geol.,73: 171-177

Lin Y, Zheng M, Ye C &, Power IM 2017. Trace and rare earth element geochemistry of Holocene hydromagnesite from Dujiali Lake, central Qinghai–Tibetan Plateau, China, Carbonates and Evaporites. DOI 10.1007/s13146-017-0395-9

Maigien R 1966. Review of Research on Laterites. Natural Resources Research IV, United Nations Educational Scientific and Cultural Organization, Paris, France, 4: 1-70

McCulloch MT & Wasserburg GJ 1978. Sm-Nd and Rb-Sr Chronology of continental crust formation: Science, 200: 1003-1011.

McLennan SM 1989. Rare earth elements in sedimentary rocks; influence of provenance and sedimentary processes In: Lipin, B.R., McKay, G.A. (eds.), Geochemistry and Mineralogy of Rare Earth Elements: *Reviews in Mineralogy, 21: 169-200.*

McLennan SM, Hemming S, McDaniel DK & Hanson GN 1993. Geochemical approaches to sedimentation, provenance, and tectonics, in Johnson, M.J., Basu, A. (eds.) Processes Controlling the Composition of Clastic Sediments: *Geological Society of America, Special Paper, 284: 21-40.*

McLennan SM, Taylor SR, McCulloch MT & Maynard JB 1990. Geochemical and Nd-Sr isotope composition of deep sea turbidites: crustal evolution and plate tectonic associations. Geochim. Cosmochim. Acta, 54: 2015-2050.

McLennan SM & Taylor SR 1991. Sedimentary rocks and crustal evolution: tectonic setting and secular trends. *J. Geol., 99: 1–21.*

Mehmet Muzaffer K 2013. Geochemistry, provenance and tectonic setting of the Late Cambrian Early Ordovician Seydişehir Formation in the Çaltepe and Fele areas, SE Turkey, Chemie der Erde – Geochemistry. 74(2):

Mishra M 2010. Geochemical signatures of Mesoproterozoic siliciclastic rocks of the Kaimur Group of the Vindhyan Supergroup, Central India, *Chinese Journal of Geochemistry. 29(1):21-32*

Mishra M & Sen S 2012. Provenance, tectonic setting and source-area weathering of Mesoproterozoic Kaimur Group, Vindhyan Supergroup, Central India. *Geologica Acta, 10(3): 283-293.*

Moradi AV, Sarı A & Akkaya P. 2016. Paleoredox reconstruction of bituminous shales from the Miocene Hançili Formation, ÇankırıÇorum Basin, Turkey: Evaluating the role of anoxia in accumulation of organic-rich shales, Marine and Petroleum Geology.76:136-150.

Nesbitt HW & Young GM 1982. Early Proterozoic climates and past plate motions inferred from major element chemistry of lutites. Nature (London), 299: 715-717

Nesbitt HW & Young GM 1984. Prediction of some weathering trends of plutonic and volcanic rocks based on thermodynamic and kinetic considerations. Geochim. *Cosmochim. Acta, 48: 1523–1534.*

Nesbitt HW & Young GM 1989. Formation and digenesis of weathering profiles. *Journal of Geology, 97: 129-147.*

Ngong NR, Agyingi CM, Foba-Tado J, Mboudou GMM, Nshukwi A & Beckley VN 2015. Sedimentology and Geochemical Evaluation of Lignite-Argillite Sequences in a Named Basin in Bali Nyonga, Northwest, Cameroon, *International Journal of Geosciences. 6(8): 917-937.*

Ngueutchoua G, Ngantchu LD, Youbi M, Ngos S III et al. 2017. Geochemistry of Cretaceous Mudrocks and Sandstones from Douala Sub-Basin, Kumba Area, South West Cameroon: Constraints on Provenance, Source Rock Weathering, Paleo-Oxidation Conditions and Tectonic Environment, *International Journal of Geosciences. 8(8):393-424*

Nwajide CS 2013. Geology of Nigeria's Sedimentary Basins. CSS Bookshops Ltd, Lagos, 565 pp.

Okezie CN & Onuogu SA 1985. The lignites of southeastern Nigeria. Geol. Survey of Nigeria Occasional Paper, 10: 28p

Omotosho O & Eze-Uzomaka OJ 2008. Optimal stabilization of deltaic laterite. *J. S. Afr. Inst.Civil Eng., 50(2): 10-17.*

Parkinson J 1907. The post-Cretaceous stratigraphy of southern Nigeria. *Q.J. Geol. Soc.London, 63: 311 – 320.*

Pettijonh FJ 1963. Chemical composition of sandstones, excluding carbonate and volcanic sands, in: Fleischer, M (ed.), Data of geochemistry: U.S. Geol. Surv. Paper, 440-S:19p.

Pundaree, Nandigama, Krishna AK, Subramanyam KSV, Sawant SS, Kavitha S, Kalpana MS,Patil DJ & Dayal AM 2015. Early Eocene carbonaceous shales of Tadkeshwar Formation, Cambay basin, Gujarat, India: Geochemical implications, petrogenesis and tectonics, Marine and Petroleum Geology. xxx:1-11.

Reijers TJA 1996. Selected Chapters on Geology: Sedimentary geology and sequence stratigraphy in Nigeria and three case studies and a field guide. SPDC Corporate reprographic Services, Warri, Nigeria, 197p.

Rimmer SM 2004. Geochemical paleoredox indicators in Devonian–Mississippian black shales, Central Appalachian Basin (USA), Chemical Geology. 206(3):373-391

Šajnović A, Grba N, Neubauer F, Grubin MK, Stojanović K, Petković N, & Jovančićević B 2019. Geochemistry of sediments from the Lopare Basin (Bosnia and Herzegovina): Implications for paleoclimate, paleosalinity, paleoredox and provenance, Acta Geologica Sinica – English Edition, https://doi.org/10.1111/1755-6724.14324

Short KC & Stauble AJ 1967. Outline of Geology of Niger Delta. AAPG Bull., 51(5): 761-779.

Taylor SR & Mclennan SM 1981. The composition and evolution of the Continental crust: rare earth element evidence from sedimentary rocks. Philosophical Transactions of the Royal Society of London, A301: 381-399.

Taylor SR & McLennan SM 1985. The Continental Crust: Its Composition and Evolution:Blackwell, Oxford, 312p.

Ugbe FC 2011. Basic Engineering Geological Properties of Lateritic Soils from Western *Niger Delta. Research Journal of Environmental and Earth Sciences, 3(5): 571-575*

Varghese TI, Nageshrao PT, Raghavendramurthy N & Ramasamy N 2018. Sediment geochemistry of coastal environments, southern Kerala, India: implication for provenance, *Arabian Journal of Geosciences. 11(3)*

Whiteman AJ 1982. Nigeria: Its Petroleum Geology, Resources, and Potentials. 1 & 2. Graham and Trotman, London, 394p.

Wilde P, Quinby-Hunt MS & Erdtmann BD 1996. The whole-rock cerium anomaly— A potential indicator of eustatic sea-level changes in shales of the anoxic facies. Sedimentary Geology, 101: 43–53.

Zeng S, Wang J, Fu X, Chen W, Feng X, Wang D, Song C & Wang Z 2015. Geochemical characteristics, redox conditions, and organic matter accumulation of marine oil shale from the Changliang Mountain area, northern Tibet, China, Marine and Petroleum Geology. 64: 203-221.